Tectonophysics
Elsevier Publishing Company, Amsterdam – Printed in The Netherlands

PALAEOMAGNETISM OF THE–UPPER GONDWANA–RAJMAHAL TRAPS, NORTHEAST INDIA*

C.T. KLOOTWIJK
Palaeomagnetisch Laboratorium, State University of Utrecht, Utrecht (The Netherlands)

(Received June 30, 1971)

ABSTRACT

Klootwijk, C.T., 1971. Palaeomagnetism of the–Upper Gondwana–Rajmahal traps, northeast India. *Tectonophysics*, 12: 449–467.

For a detailed palaeomagnetic investigation, oriented cores were drilled from the tholeiitic Rajmahal traps basalts (northeast India), which are of a Late Mesozoic age. In total 183 samples were collected from 27 sites spread over the whole trap area. Two sites appeared to be reversely magnetized.

Alternating field and thermal demagnetization resulted in a mean direction $D = 314.5°, I = -64.5°$ ($k = 60$, $a_{95} = 3.5°$; 25 sites), which corresponds to a virtual geomagnetic pole position: 63° W, 7° N ($dp = 4.5°$, $dm = 6°$)

INTRODUCTION

The present paper contributes to a series of reports, presenting results from palaeomagnetic sampling expeditions on the Indian subcontinent during the winter seasons 1966–1967 and 1968–1969 (Wensink, 1968; Wensink and Klootwijk, 1968; Wensink and Klootwijk, 1971). The field trips were made by a group from the State University of Utrecht guided by the Geological Survey of India.

Volcanic rocks of Late Mesozoic age, i.e., Rajmahal traps and associated dykes and sills, are the oldest and possibly the only igneous rocks in the mainly sedimentary Gondwana sequence (Late Carboniferous to Middle Cretaceous) on the Indian subcontinent.

Apart from sediments of the Upper Vindhyan series, for which an Early Palaeozoic age has been suggested, no Palaeozoic rocks are present on the subcontinent that are older than the Gondwana sediments (Fig.1). Moreover, preliminary results from the present author point to some remagnetization of Gondwana sediments during the Early Tertiary by Deccan traps activity (Klootwijk, in preparation).

In view of these facts it is clear that an accurate determination of the pole position for the Rajmahal traps basalts is of a key importance in defining the apparent polar wandering path of the Indian subcontinent.

Several workers have paid attention to the palaeomagnetism of the Rajmahal traps (Clegg et al., 1958; McDougall and McElhinny, 1970; Radhakrishnamurty, 1970). Only Radhakrishnamurty and McElhinny used cleaning techniques. The results from Radhakrishnamurty produce a pole that diverges towards the present pole position by about 11° compared

* This paper forms part of a doctoral thesis.

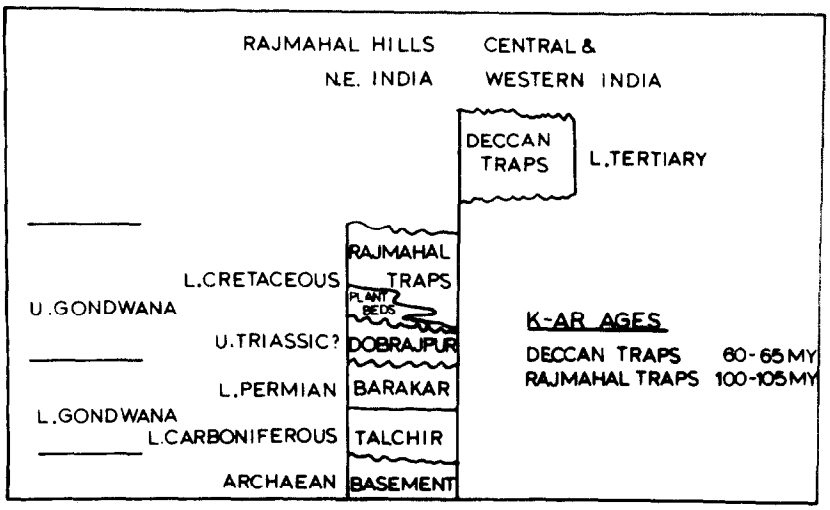

Fig.1. Schematic view of Rajmahal Hills stratigraphy.

with McElhinny's results. McElhinny's results are based upon a small number of samples (16) from only 4 localities.

As a part of the studies on the Indian apparent polar wandering curve, an extensive collection of 183 samples from 27 sites in the Rajmahal Hills was gathered. The sites were widely spread over the trap area so as to minimize the risk of possible errors due to slight (if any) tectonic influence (Fig.2).

GEOLOGICAL SITUATION

During the Gondwana period, from Late Carboniferous to the Middle Cretaceous, sediments were deposited in India under predominantly fluviatile and lacustrine conditions. These beds are preserved in a mostly undeformed and unmetamorphosed state in a number of downfaulted troughs in northeast India.

Based on palaeontological evidence, the Gondwana system is usually divided into a Lower Gondwana sequence (*Glossopteris* flora) and an Upper Gondwana sequence (*Ptilophylum* flora), the latter including the Rajmahal traps.

These traps in West Bengal and Bihar (northeast India) are the only major exposures of volcanic rocks in the Indian Gondwana sequence. Together with the Deccan traps in central and western India, the Rajmahal traps belong to the plateau type of tholeiitic basalts. Recent K/Ar determinations have assigned ages of minimal 60–65 m.y. (Early Palaeocene) to the Deccan traps (Wellmann and McElhinny, 1970) and 100–105 m.y. (Early Cretaceous) to the Rajmahal traps (McDougall and McElhinny, 1970). The latter K/Ar age is in agreement with recent palynological evidence stating a probable age from Late Jurassic to Early Cretaceous, as quoted by McDougall and McElhinny (1970).

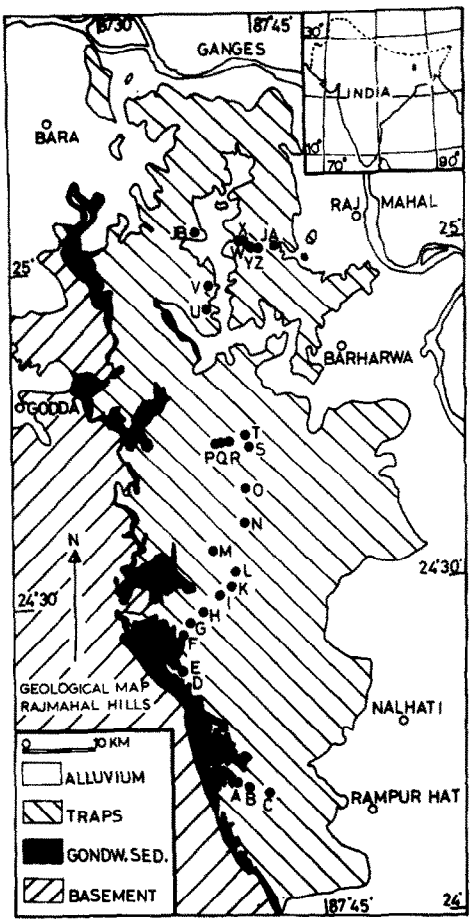

Fig.2. Geological sketch map of the Rajmahal Hills. Dots represent sampling sites, labeled as in Table I.

The Rajmahal stage consists of a sequence of at least 600 m of basaltic lava flows of uniform composition, and inter-trappean carbonaceous shales and sandstones up to a total thickness of 35 m.

At least ten distinct flows, ranging in thickness from 20 to 75 m, have been mapped by Hobson (1929), but the total number of flows must be much larger (Pascoe, 1959, p.979).

Some faulting has been reported (Ball, 1876), but the traps are essentially horizontal, overlapping slightly unconformably on coarse-grained sediments of the Dobrajpur stage (assumed to be of a Late Triassic age), on Lower Gondwana sediments and on the metamorphic basement (Fig.1,2).

A laterite cap has developed in the eastern trap area; here the traps are plunging with a negligible dip below the Ganges alluvium.

SAMPLING

The trappean structure is less well developed in the Rajmahal Hills (northeast India) than in the Deccan traps of the Western Ghats (western India). This hampered us in sampling sequences of separate flows as was done in the Deccan traps (Wensink and Klootwijk, 1971).

Over short distances we could generally discern no more than three separate flows in succession; correlation over greater distances was not possible. We could therefore not position the separate flows into an ideal stratigraphic column.

The sites were chosen in road exposures and stream beds. Eight samples per site were drilled, by means of a portable drill. Orientation was performed by a normal compass and a clinometer, using a specially designed orientation apparatus. Distance from the rocks to the compass was at least 20 cm. As the mean intensity of N.R.M. was about $2 \cdot 10^{-3}$ e.m.u./cm^3, it may be safely assumed that no orientation error crept in due to the rocks own magnetization.

LABORATORY TREATMENT

The N.R.M. of 325 specimens, 2.5 cm diameter, 22 cm height, was measured on the astatic magnetometers of the palaeomagnetic laboratory, State University of Utrecht, The Netherlands. From each site about six specimens were chosen for demagnetization. One or two specimens of each site were progressively demagnetized in 14 – 22 steps up to peak values of 500–2000 Oe. The remaining specimens were partially progressively demagnetized in 5 – 10 steps.

Several pilot samples were thermally demagnetized in 16 progressive steps up to 600°C (for a description of the furnace, see Mulder, 1970). The remanence was measured between each step after the specimens had cooled down to room temperature.

METHOD OF ANALYSIS

The results are interpreted essentially according to the methods described by Zijderveld (1967). The basic computations were programmed in ALGOL-60 by the present author and were carried out on the Philips Electrologica X-8 computer of the Electronical Computer Centre, State University Utrecht.

Directional analysis was based upon computer plots of orthogonal projection figures (Zijderveld, 1967). Characteristic directions were determined from the best-fitting single component trajectory, i.e., a straight line in the demagnetization figures. These trajectories were determined both with standard methods (Zijderveld, 1967) as well as with a least-square approximation procedure.

Density distribution projections, a normal tool in petrofabric analysis, showed to be of great visual aid in palaeomagnetism (Van der Voo, 1969). For this reason a computing program was devised according to the basic concepts of Noble and Eberly (1964), Siemens (1967) and Möckel (1969).

An ALGOL-procedure, programmed by Van den Ende (1971) delivering the orientation of palaeoisoclines, was used in a plot program.

RESULTS

The intensity of initial remanence ranged between $2 \cdot 10^{-4}$ and $6 \cdot 10^{-2}$ e.m.u./cm^3, with a mean intensity of $2 \cdot 10^{-3}$ e.m.u./cm^3. The intensity of induced magnetization (H_z = 0.44 Oe) ranged between $9 \cdot 10^{-5}$ and $2 \cdot 10^{-3}$ e.m.u./cm^3, with a mean value of $4 \cdot 10^{-4}$ e.m.u./cm^3. So the initial Q-values generally greatly exceed unity, ranging from about 1 to 10^3 (Table I).

A density distribution of initial N.R.M. directions shows a mean northwest-oriented direction pointing upwards. A streaking towards the present field, at the sampling locality dipping 30° downwards, is clearly visible (Fig.3A, B). Initial site mean directions are rather scattered in the northwest quadrant pointing upwards (Fig.4A).

By A.F. treatment two magnetic components could be distinguished; a secondary present field component and an accurately determinable characteristic component. The former soft magnetic component was completely removed during A.F. treatment at 200–250 Oe peak value (e.g., Fig.6A, C, D.).

On the grounds of their behaviour during A.F. treatment the specimens from various sites could be divided into two types:

(1) The first type showed a very fast decrease in total intensity in fields up to 250 Oe. The secondary ambient field component was then completely removed, the characteristic component only partly. Less than 10% of the initial intensity remained at 250 Oe (Fig.5A, B and 7).

(2) The second type showed a more stable magnetization. The decrease in intensity was regular and slower than Type-1 specimens. A small secondary present field component was broken down completely in fields less than 200 Oe. The remaining intensity at 200–250 Oe exceeds 20% of the initial intensity (Fig.6 and 7).

Demagnetization figures from specimens from the southernmost sites IRAA, IRAD and IRAI were less regular and this may be due to the somewhat weathered condition of samples from these sites. However, in all samples all over the trap area accurate characteristic directions could be determined, certainly in using the least-square fitting procedure. The demagnetization diagrams from specimens from several sites showed a slight scatter in measuring points, a least-square fitting procedure was applied to the measurements from these specimens in order to obtain a direction fitting well to the data.

Characteristic directions determined from thermal demagnetization procedures agree with the A.F. demagnetization results (Fig.8). Secondary ambient field components were removed beneath 200–300°C. The blocking range of the characteristic component is rather low, 200–400°C (Fig.9).

The cleaning procedures yielded close-grouped site-mean directions (Fig.3, 4 and Table I). The resulting mean direction was $D = 314.5°$, $I = -64.5°$, $a_{95} = 3.5°$ (25 sites, 2 sites discarded; IRAB, IRAQ).

TABLE I

Magnetization, demagnetization and pole position data for Rajmahal traps basalt specimens

Site	Samples[*1]	Natural remanent magnetization								After
		Specimens[*2]	Mean-site	Direction	k	a_{95}[*3]	Intensity[*4]	Induced[*4]	Q-value[*4]	Mean-s
IRAA	8	9(7)	336	+16.5	2.5	–	17– 41	6–22	2– 11	317
IRAB	8	9(6)	339	– 2.5	122	6	51– 74	15–17	7– 10	326.5
IRAC	8	15(7)	60.5	+86.5	38	10	11– 35	9–16	2– 5	166.5
IRAD	8	14(6)	140.5	–30	48	9.5	12– 18	18–23	1– 2	293.5
IRAE	8	11(7)	2.5	+81.5	19	14	6– 17	7–12	1– 5	134
IRAF	8	16(6)	307.5	–43.5	33	12	4– 5	6– 9	1– 2	305.5
IRAG	8	13(6)	331	–36	5	34	71–177	8–21	2– 19	300.5
IRAH	8	15(7)	338	–46.5	9.5	20.5	16– 24	7–14	3– 6	316.5
IRAI	8	16(7)	297	–14	4.5	32.5	3– 23	9–14	3– 17	274
IRAK	7	14(6)	303	–66	115	2	12– 16	13–21	2– 6	289.5
IRAL	8	15(6)	297	–62.5	108	6.5	20– 84	8–10	2– 3	298.5
IRAM	8	14(6)	341.5	–65	9	24	19– 45	9–13	3– 4	327
IRAN	8	16(6)	346.5	–34.5	61	8.5	10– 15	8–10	2– 3	331
IRAO	7	9(6)	349	– 8	25	13.5	16– 19	9–13	3– 4	323
IRAP	8	15(6)	325	–47	47	10	20– 50	10–15	4– 9	299
IRAQ	8	12(9)	197	–18.5	9	18	48–309	7–14	11– 78	180.5
IRAR	8	14(7)	283	–25.5	69	7.5	66–593	10–16	14–1052	314
IRAS	7	14(6)	300.5	–30.5	387	3.5	48– 59	9–11	10– 14	300.5
IRAT	7	14(6)	282.5	–47.5	7.5	26.5	16– 46	9–12	3– 10	289.5
IRAU	2	4(4)	305	–58	454	4.5	78–110	7–12	15– 29	323.5
IRAV	4	8(6)	290.5	–20.5	290	20.5	65–117	11–16	10– 26	321
IRAW	5	7(6)	326	–66	1315	2	51– 58	4– 5	23– 28	321
IRAX	5	9(5)	329.5	–62.5	57	10	5– 60	6–12	11– 21	320
IRAY	6	11(6)	247	–59.5	50	9.5	4– 21	3– 5	2– 7	346
IRAZ	6	11(6)	323.5	–44.5	39	11	8–351	7–10	2– 4	313.5
IRJA	5	7(6)	331.5	–59	83	7.5	316–461	7–18	57–1012	323.5
IRJB	2	4(4)	323	–46	78	10.5	10– 12	7– 8	3– 4	323

All directional data and angular values are denoted in degrees.

[*1] During the transport some samples were lost, so several sites are incomplete.

[*2] Number of specimens measured for N.R.M., between brackets number of specimens selected for demagnetization treatment.

[*3] Only the specimens selected for demagnetization treatment are used in determining the semi-angle of Fischer's cone of confidence.

demagnetization							Pole position data		
Direc-tion	Specimens[*5]	Method[*6]	k	a_{95}	Corresponding direction at Nagpur[*7]		Pole position	dp	dm
−53.5	7	LS	31	11	309	−50	−56° W +19° N	10.5	15
−40	6	LS	96	7	321	−28.5	−51° W +37° N	4.5	7.5
+74	7	ST	230	4	148.5	+74	−86.5°W + 5° N	6.5	7
−56.5	5	LS	529	3.5	295	−50.5	−49° W + 8.5°N	5.5	7.5
+77	6	ST	561	3	117	+74.5	−52° W + 3.5°N	5	5
−64.5	6	ST	194	5	295.5	−60.5	−58° W + 3.5°N	6	7.5
−66	4	LS	520	4	291	−61.5	−57.5°W + 0° N	5.5	6.5
−62.5	7	ST	234	4	306.5	−59.5	−62.5°W +11° N	5	6
−68.5	7	ST	295	11.5	267	−62.5	−52° W −16.5°S	16	19
−71.5	6	ST	1605	1.5	279.5	−67	−60° W −10° S	2.5	3
−68.5	6	ST	2915	4	289	−64	−59.5°W − 3.5°S	5.5	6.5
−63	5	LS	293	4.5	315.5	−61.5	−68.5°W −14.5°S	5.5	7
−59	6	LS	3025	1	320.5	−58	−69° W +20° N	1.5	2
−63	6	ST	260	4	312	−61	−66° W +13° N	5	6.5
−64.5	5	ST	200	5.5	289.5	−59.5	−55° W + 0° N	7	8.5
−14	9	ST	10	17.5	178	− 7	−94.5°W +72° N	9	17.5
−68	5	ST	75	9	302	−65.5	−65.5°W + 4° N	12.5	15
−58.5	6	LS	572	3	298	−53.5	−50° W + 5° N	3	4
−84	6	ST	12	20	289	−80	−80° W −20° S	39	39.5
−58	4	ST	1545	2.5	314	−56	−63.5°W +17.5°N	2.5	3.5
−51	6	ST	86	7	313	−48	−57° W +22° N	6.5	9.5
−66	6	LS	1745	1.5	309	−63.5	−67° W + 9° N	2	2.5
−65	5	ST	141	6.5	308	−62.5	−64° W + 9.5°N	8.5	10.5
−68.5	6	ST	1415	2	331.5	−69	−83.5°W +12.5°N	2.5	3
−49	6	ST	1660	1.5	305.5	−45	−50.5°W +19° N	1.5	2
−61	5	ST	220	5	312.5	−59	−65° W +15° N	6	8
−56.5	4	LS	915	3	313.5	−54.5	−62° W +18.5°N	3	4.5

[*4] Intensity: range of initial remanent magnetization per site in 10^{-4} e.m.u./cm^3. Induced: range of initial induced magnetization per site in 10^{-4} e.m.u./cm^3. Q-value: range of Q-values per site.

[*5] Number of demagnetized specimens, used for determination of individual site-mean directions.

[*6] Method used for the determination of characteristic direction: LS = least-square approximation; ST = standard methods (see Zijderveld, 1967).

[*7] Corresponding direction at Nagpur (21.06° N, 79.23° E), according to the dipole hypothesis.

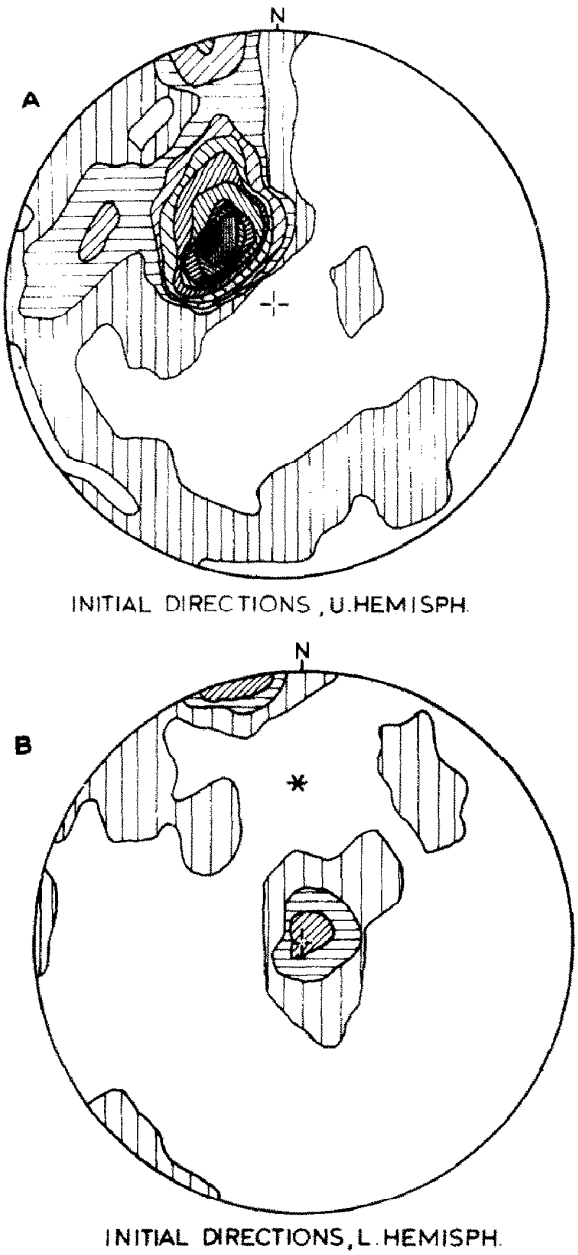

Fig.3. A. Density distribution of initial directions in equal area projection, counted with a 2% circle. Upper hemisphere projection only. B. Idem, lower hemisphere projection only. C. Density distribution of characteristic directions in equal area projection, counted with a 1% circle. Upper hemisphere only.

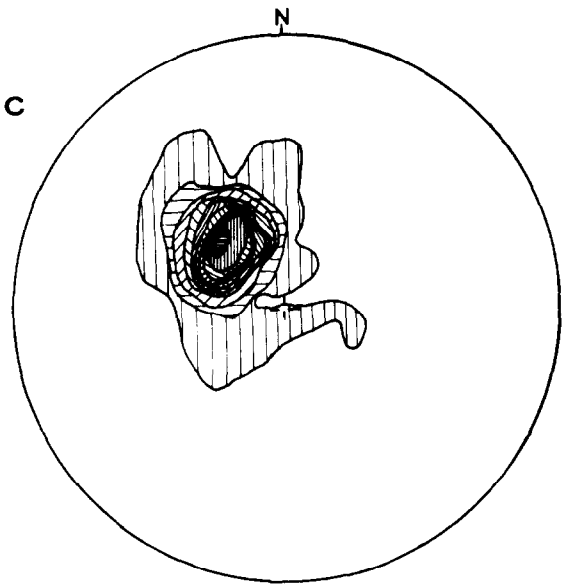

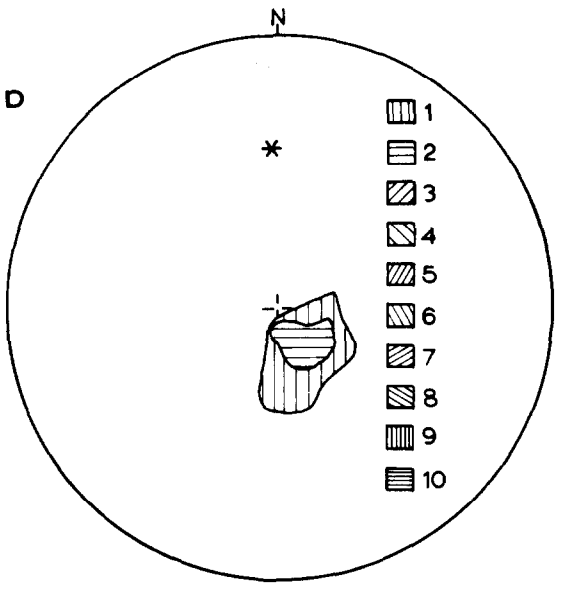

D. Idem, lower hemisphere projection only. Unit weight was given to specimen directions in all density distribution histograms. Contouring density:

symbol:	*1*	*2*	*3*	*4*	*5*	*6*	*7*	*8*	*9*	*10*	
A, B	2.7	5.4	8.2	10.9	14.3	17	19.7	22.5	25.2	27.9	%
C, D	4	7,4	11.4	14.7	18.8	22.8	26.2	30.2	33.5	37.5	%

* = Earth field direction, dipping downwards at the sampling locality.

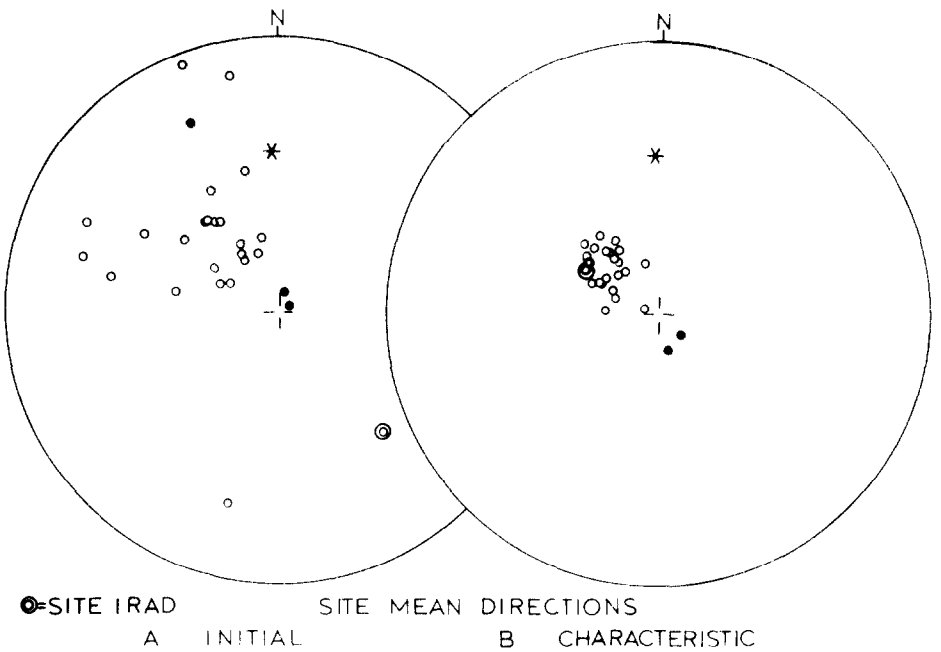

Fig.4. A. Stereographic projection of initial site mean directions. B. Stereographic projection of characteristic site mean directions. Legend: ○ = directions pointing upwards; ● = directions pointing downwards; ★ = local direction of the earth magnetic field.

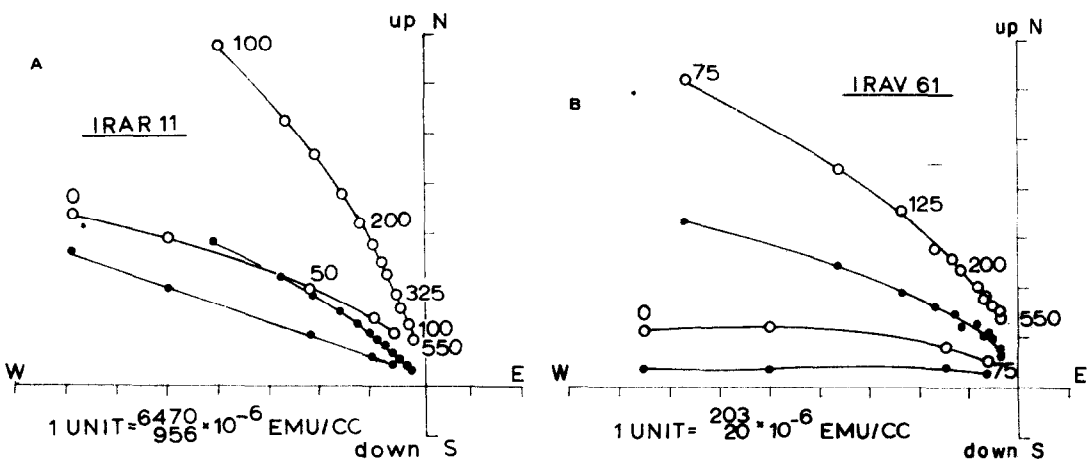

Fig.5. A.F. demagnetization diagrams for Type-1 specimens IRAR11 and IRAV61. Because of the fast decrease in intensity of N.R.M. during demagnetization treatment, different scaling factors were applied for separate parts of the demagnetization graph. The separate parts of the demagnetization graph are plotted in one figure. These scaling factors are for instance in Fig.5A: $6470 \cdot 10^{-6}$ for the trajectory between 0 and 100 Oe peak value and $956 \cdot 10^{-6}$ for the trajectory between 100 and 550 Oe peak value. General explanation for demagnetization diagrams (A.F. and thermal): plotted points represent successive positions in orthogonal projection of the end points of the magnetic vector; closed circles represent projections on the horizontal plane; open circles represent projections on the east-west vertical plane; numbers denote peak values of demagnetizing field in Oersteds (Oe) or furnace temperatures in °C. For several samples composite figures had to be drawn (Fig.5, 8, 10).

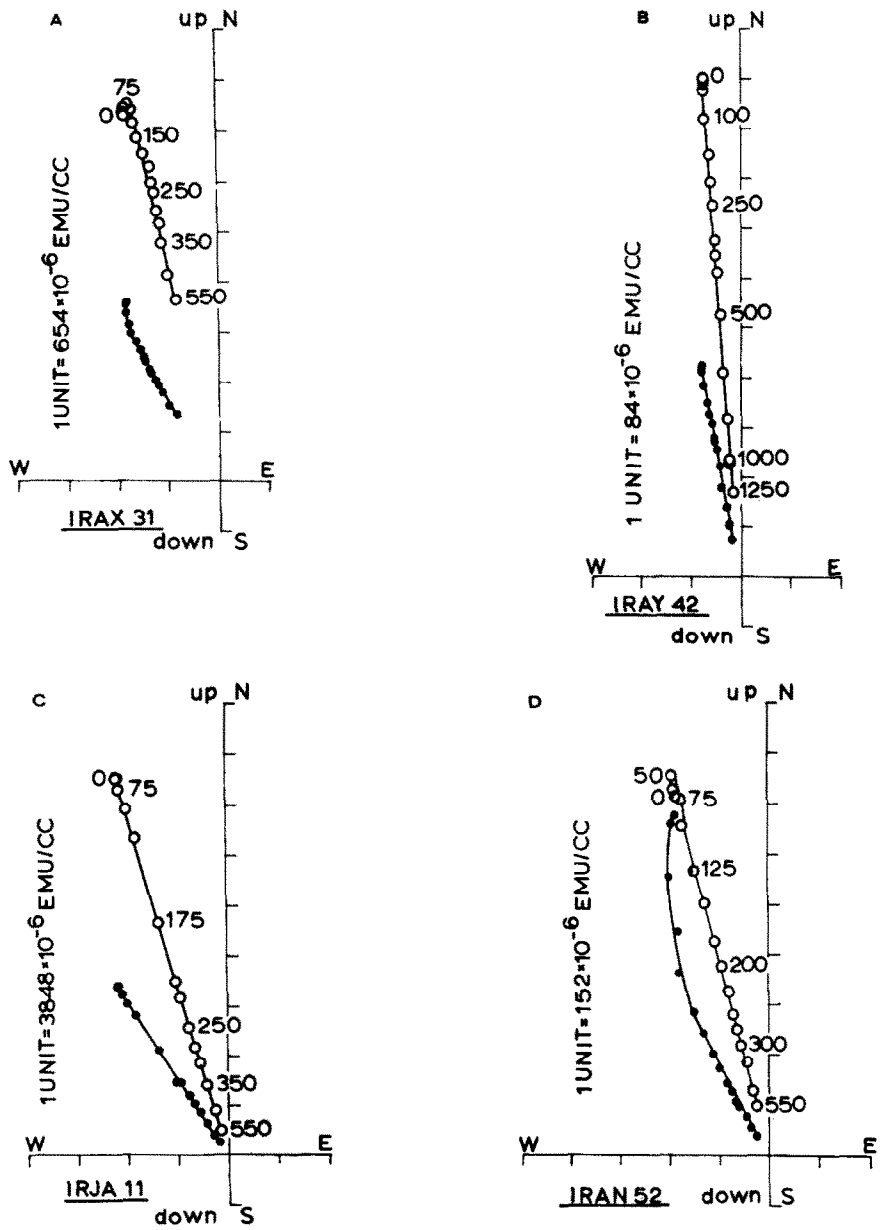

Fig.6. A.F. demagnetization diagrams, Type-2 specimens IRAX31, IRAY42, IRJA11, IRAN52. Legend: as for Fig.5.

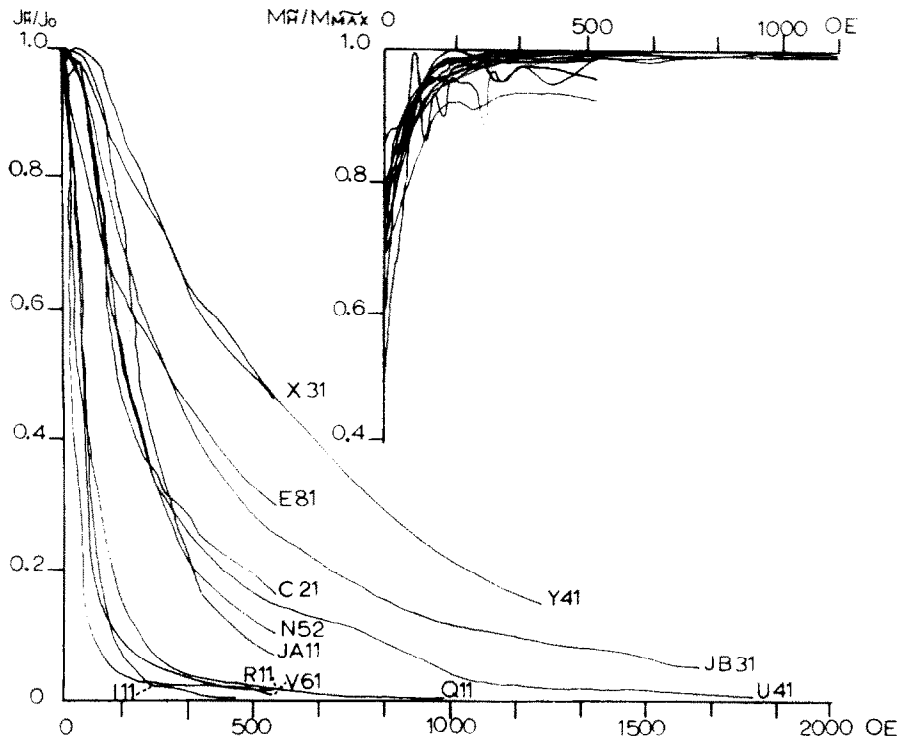

Fig.7. Normalized plots showing the decrease in total intensity of remanent magnetization (J_H) and the general increase in intensity of induced magnetization (M_H) during the progressive A.F. demagnetization. J_O = initial intensity of remanent magnetization; M_{max} = maximum value of induced magnetization obtained during the progressive A.F. demagnetization procedure. The continuous lines in the figure do connect separate experimental values of J_H and M_H at peak values of 0, 25, 50,75, 100, 125, 150, 175, 200, 225, 250, 275, 325, 375, 450, 550, 650, 750, 850, 1000, 1250, 1400, 1600, 1800 Oe; the points themselves are omitted in this figure for reason of visibility. Type-1 specimens (IRAI11, IRAQ11, IRAR11, IRAV61) and Type-2 specimens can be discerned.

Sites IRAC and IRAE (Type 2) were reversely magnetized, compared with the remaining sites (Fig.6, 8). During A.F. treatment, stable close-grouped characteristic directions were determined after elimination of a soft ambient field component at 250–275 Oe. (Fig.7) IRAC; $a_{95} = 4°$, IRAE; $a_{95} = 3°$. However, the inclination at the reversed sites was somewhat steeper than the mean inclination at the normal sites.

All specimens from site IRAD showed an initial close-grouped direction with a southeast direction, pointing upwards. A soft southeast-directed component of strong intensity could already largely be eliminated in fields of 75 Oe and was completely removed at 250 Oe peak value (Fig.10). It is presumed that this soft component was induced by the overlying reversely magnetized flow IRAE. On the other hand, the harder characteristic magnetization directions

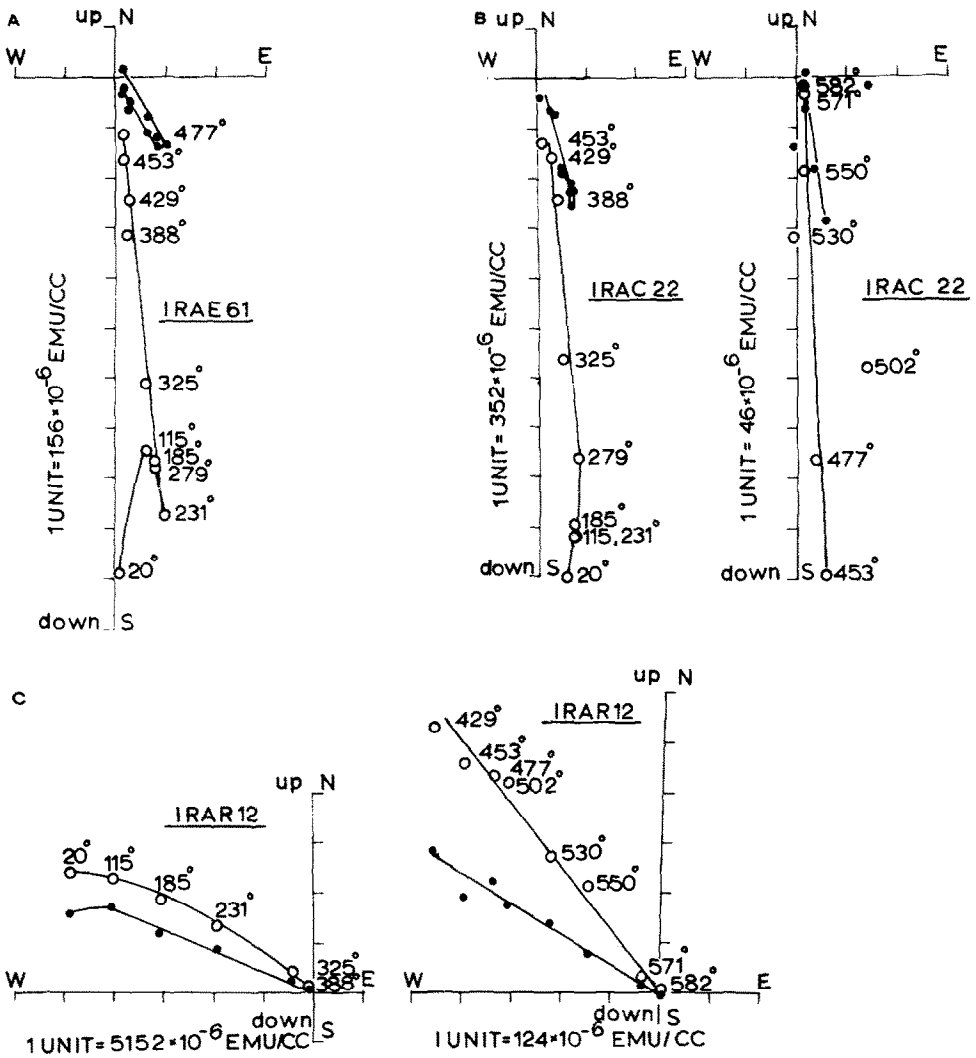

Fig.8. Thermal demagnetization diagrams. A. Specimen IRAE61; B. Specimen IRAC22 (2 diagrams); C. Specimen IRAR12 (2 diagrams). Legend: as for Fig.5; numbers denote furnace temperatures in °C.

of site IRAD are close-grouped (a_{95} = 3.5°) and in good accordance with the mean trap direction (Table I, Fig.4).

Sites IRAB and IRAQ have been discarded. The stable low inclination direction of site IRAB may represent a transitional direction (Table I).

An increase in bulk susceptibility was noted during A.F. treatment. Stacey (1960) ascribes such an increase to "the alignment of random domain directions in multi-domain grains into the nearest easy direction of magnetization of crystals to the field direction".

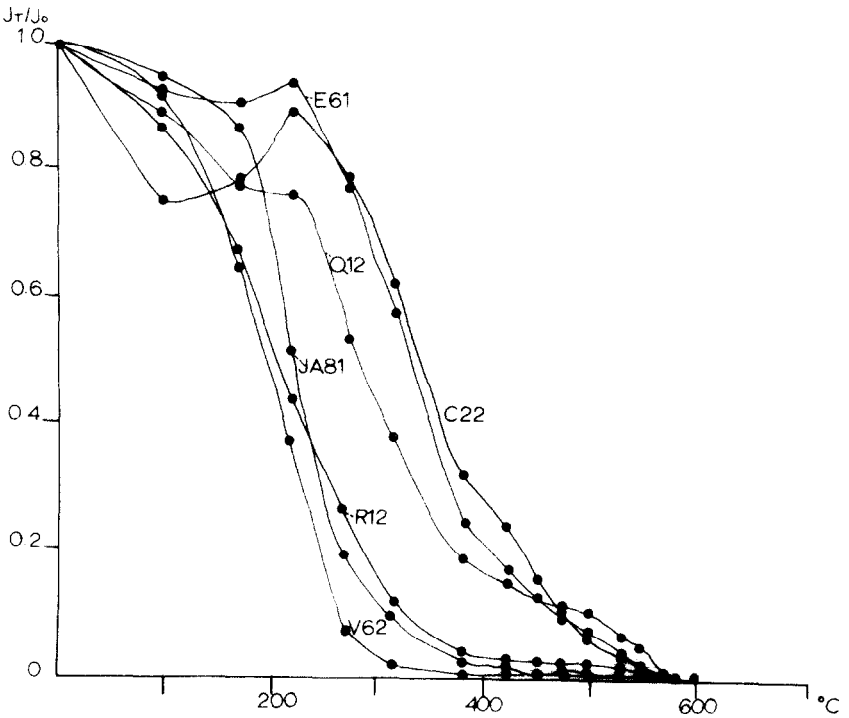

Fig.9. Curves showing the normalized intensities of natural remanent magnetization during thermal demagnetization of normal (IRAQ12, IRAR12, IRAV62, IRJA81) and reversely (IRAC22, IRAE61) magnetized specimens.

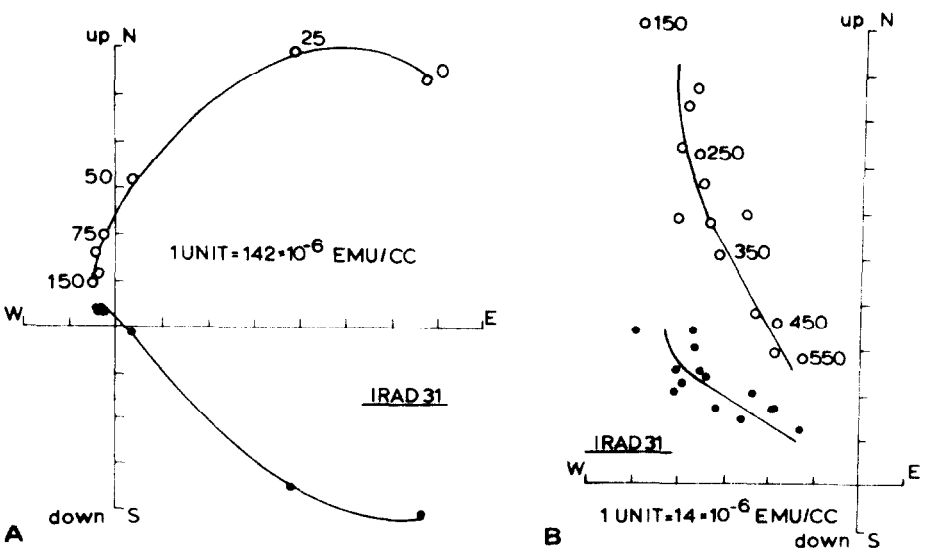

Fig.10. A.F. demagnetization graphs from specimen IRAD31. The trajectory represented in B is the extension of the trajectory represented in A. Because of the very fast decrease in intensity during demagnetization, the scale of the second figure had to be enlarged about ten times. The small intensity of N.R.M. is responsible for the slight spread in measuring positions in B.

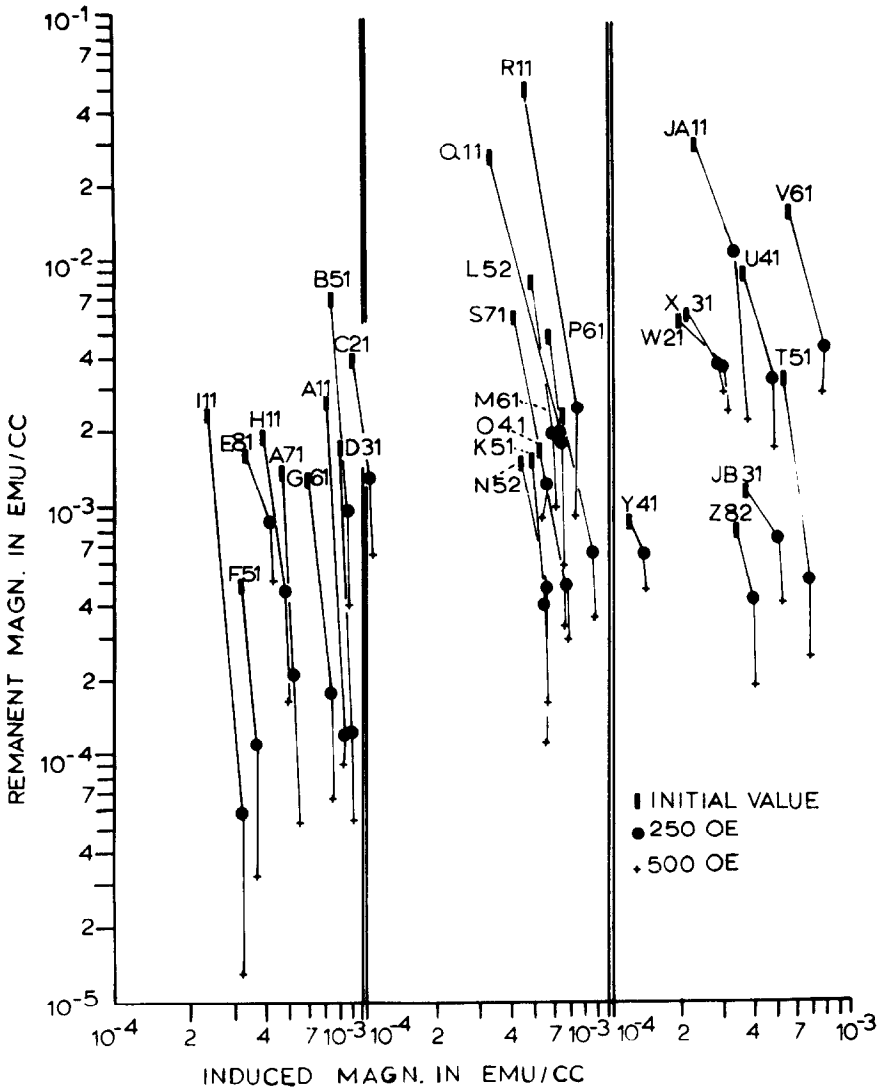

Fig.11. Double logarithmic plot representing the intensity of remanent magnetization against the intensity of induced magnetization. From all values measured during progressive A.F. demagnetization, only the initial value and the values measured after treatment in 250 and 500 Oe are represented. Note the general lack of increase in induced magnetization after A.F. demagnetization in 250 Oe peak value. The ordinate is tripartite in order to distinguish separate specimens.

However, such a tendency does not seem to fully explain the effect we noticed.

An important effect seems to be that the increase in susceptibility is generally the stronger the greater the decrease in remanent magnetization (Fig.11). The increase in susceptibility is mainly observed during treatment with alternating fields of lower intensity (less than 250

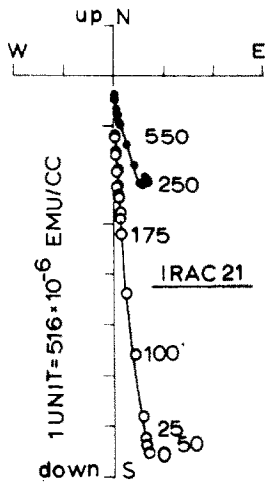

Fig.12. A.F. demagnetization diagram, reversely magnetized Type-2 specimen IRAC21. Legend: as for Fig.5.

Oe peak value), when the secondary components are being removed (Fig.5–12). So the increase in susceptibility may partly be attributed to a decrease in relaxation time of domains contributing to the viscous magnetization.

CONCLUSIONS

The cleaning effect of the A.F. treatment is very pronounced when we consider the density distribution of initial and characteristic directions (Fig.3).

The resulting mean direction (25 sites) is $D = 314.5^\circ$, $I = -64.5^\circ$, $a_{95} = 3.5^\circ$. This direction fits nicely in between the results from McElhinny ($D = 310^\circ$, $I = -67^\circ$) and those from Radhakrishnamurty ($D = 323^\circ$, $I = -64^\circ$), more closely approaching the former direction (Fig.13, Table II).

In comparing Radhakrishnamurty's pole position with McElhinny's results and the present one, it is clear that Radhakrishnamurty's pole diverges slightly towards the present pole (Fig.13). Therefore, although Radhakrishnamurty applied A.F. and thermal cleaning methods, it seems that his results had perhaps not been entirely cleaned from a present field component. McElhinny's results may suffer a small inaccuracy because 16 samples were gathered from 4 localities only.

However, the divergence in the poles obtained by Radhakrishnamurty, McElhinny and the present author is not very pronounced (Fig.13, Table II).
All three authors obtained a spread in pole positions from individual sites exceeding the divergence in the resulting virtual pole positions.

For this reason, as the best fitting pole position I suggest the mean pole from a combination of the present results (25 sites), McElhinny's results (8 sites) and Radhakrishna-

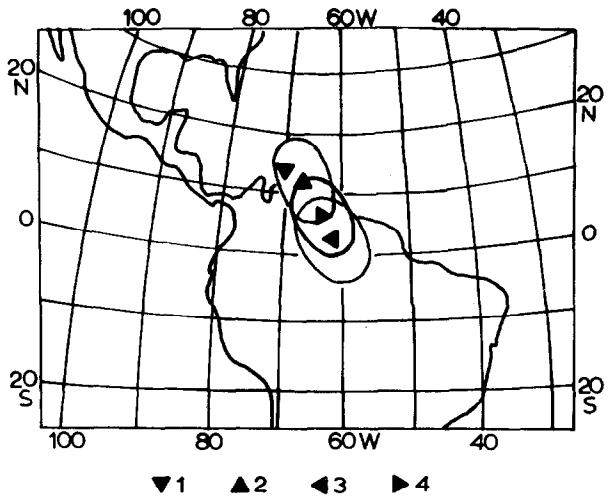

Fig.13. Western hemisphere map, showing virtual geomagnetic N-pole positions (triangles) as obtained from individual studies on the Rajmahal traps (Table II). Legend: *1* = virtual geomagnetic pole position obtained by Clegg et al. (1958); *2* = idem, Radhakrishnamurty (1970); *3* = idem. McElhinny (1970); *4* = idem, present author. Ovals of confidence are outlined for the latter three results.

TABLE II

Comparison of site mean directions

Author	Sites	Samples	Direction	k	a_{95}*	Pole position**	dp**	dm**
Clegg et al. (1958)	3	17	328 –64	–	a_{50}:2	13°N 70°W	–	–
Radhakrishnamurty (1970)	15	120	323 –64	–	4	12°N 67°W	5	6.5
McDougall and McElhinny (1970)	8	16	310 –67	187	4	3°N 62°W	5.4	6.5
Present author (1971)	25	158	314.5–64.5	60	3.5	7°N 63°W	4.5	6
Combined result, excepting Clegg et al. (1958)	48	294	316 –65	85	2.5	7.5°N 63.5°W	3	3.5

All directional data and angular values are denoted in degrees.

* Unity assigned to site directions.

** As computed by the present author from original data.

murty's results (15 sites). From this mean pole position a map of palaeolatitudes during the Rajmahal period has been plotted (Fig.14).

The resulting virtual pole position is: 7.5°N 63.5°W; this position fits very well with the results obtained by the present author: 7°N 63°W.

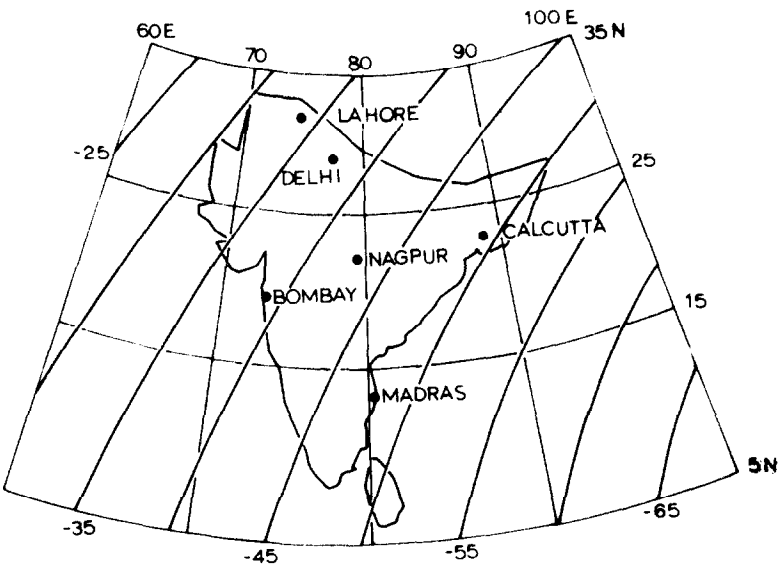

Fig.14. Map of palaeolatitudes during the Rajmahal period in stereographic projection. Redrawn from computer plot.

ACKNOWLEDGEMENTS

The present study was made under supervision of the late Prof. M.G. Rutten and Prof. J. Veldkamp, during a scholarship from the Netherlands Organisation for the Advancement of Pure Research (Z.W.O.). This organisation also financed the field trip in the winter season 1968–1969 and provided funds for carrying out the measurements. I feel greatly indebted to the late Prof. M.G. Rutten who proposed and stimulated palaeomagnetic research in the Indian subcontinent. I highly appreciate the stimulating interest of Prof. J. Veldkamp, Dr. J.D.A. Zijderveld and Dr. F.G. Mulder of the palaeomagnetic laboratory "Fort Hoofddijk" and I thank them for critically reading the manuscript. A special word of thanks is due to Dr. H. Wensink of the Geological Department, State University of Utrecht, who directed the author during the field trips. I also thank the members of the Geological Survey of India for their helpful discussions and assistance in the field, especially Dr. P.K. Dutta who guided the group during the greater part of the 1968–1969 field trip.

REFERENCES

As, J.A., 1960. Instruments and measuring methods in palaeomagnetic research. *Meded. Verh., K.N.M.I.*, 78: 56 pp.

As, J.A. and Zijderveld, J.D.A., 1958. Magnetic cleaning in palaeomagnetic research. *Geophys. J.*, 1: 308–319.

Athavale, R.N. and Verma, R.K., 1970. Palaeomagnetic results on Gondwana dykes from the Damodar Valley coal fields and their bearing on the sequence of Mesozoic igneous activity in India. *Geophys. J.* 20 (3): 303–316.

Athavale, R.N., Radhakrishnamurty. C. and Sahasrabudhe, P.W., 1963. Palaeomagnetism of some Indian rocks. *Geophys. J.*, 7: 304–313.

Athavale, R.N., Verma, R.K., Bhalla, M.S. and Pullaiah, G.P., 1970. Drift of the Indian subcontinent, since Precambrian times. In: S.K. Runcorn (Editor), *Palaeogeophysics.* Academic Press, London, pp. 291–305.

Ball, V., 1876. Geology of the Rajmahal Hills. *Mem. Geol. Surv. India.*, 13: 155–248.

Clegg, J.A., Radhakrishnamurty, C. and Sahasrabudhe, P.W., 1958. Remanent magnetism of the Rajmahal Traps of northeastern India. *Nature*, 181: 830–831.

Desmukh, S.S., 1964. Geology of the area around Taljhari and Berhait, Rajmahal Hills, Santhal Parganas, Bihar, with a discussion on the differentiation trends in the Rajmahal Traps. *Proc. Int. Geol. Congr., (22nd, New Delhi)* 7: 61–84.

Hobson, G.V., 1929. General report. *Rec. Géol. Surv. India.*, 62: 145–146.

Klootwijk, C.T., 1971. *A simulation plot program for density distribution determination, (ALGOL-60).* Int. Rep., "Fort Hoofddijk", 12 pp.

Klootwijk, C.T., *Palaeomagnetism of some Indian rocks.* Thesis, State University of Utrecht, (in preparation).

Krishnan, M.S., 1968. *Geology of India and Burma.* Higginbothams, Madras, 536 pp. (5th edition).

McDougall, I. and McElhinny, M.W., 1970. The Rajmahal Traps of India. K–Ar ages and palaeomagnetism. *Earth Planet. Sci.Lett.*, 9: 371–378.

Möckel, J.R., 1969. Structural petrology of the garnet peridotite of Alpe Arami (Ticino, Switzerland). *Leidse Geol. Meded.*, 42: 89–103.

Mulder, F.G., 1971. Palaeomagnetic research in some parts of central and southern Sweden. *Sver. Geol. Unders., Ser.C: Avh. Uppsat.*, 655: 56 pp.

Noble, D.C. and Eberly, S.W., 1964. A digital computer procedure for preparing beta diagrams. *Am.J. Sci.*, 262: 1124–1129.

Pascoe, E.H., 1959. *A Manual of the Geology of India and Burma, 2.* Government Press, Delhi, 1343 pp. (3rd edition).

Radhakrishnamurty, C., 1970. Laboratory studies for ascertaining the suitability of rocks for palaeomagnetism. In: S.K. Runcorn (Editor), *Palaeogeophysics.* Academic Press, London, pp. 235–241.

Raja Rao, C.S. and Purushottam, A., 1963. Pitchstone flows in the Rajmahal Hills, Santhal Parganas, Bihar. *Rec. Géol. Surv. India.*, 91 (2): 341–348.

Siemens, H., 1967. Ein Rechenprogramm zur Auswertung von Röntgen-Textur Goniometer Aufnahmen. *Neues Jahrb. Mineral Monatsh.*, 49–60.

Stacey, F.D., 1960. Magnetic anisotropy of igneous rocks. *J. Geophys. Res.*, 65 (8): 2429–2442.

Van den Ende, C., 1971. *A Rotation Procedure for Palaeoisocline Determination, (ALGOL-60)* Int. Rep., "Fort Hoofddijk", 4 pp.

Van der Voo, R., 1969. Palaeomagnetic evidence for the rotation of Spain. *Tectonophysics.*, 7 (1): 5–56.

Wadia, D.N., 1953. *Geology of India.* MacMillan, London, 532 pp (3rd edition).

Wellmann, P. and McElhinny, M.W., 1970. K-Ar. age of the Deccan Traps, India. *Nature*, 227: 595–596.

Wensink, H., 1968. Palaeomagnetism of some Gondwana red beds from Central India. *Palaeogeogr., Palaeoclimatol., Palaeoecol.*, 5: 323–343.

Wensink, H. and Klootwijk, C.T., 1968. The palaeomagnetism of the Talchir series of the Lower Gondwana system, central India. *Earth Planet. Sci. Lett.* 4 (3): 191–196.

Wensink, H. and Klootwijk, C.T., 1971. Palaeomagnetism of the Western Ghats, south of Poona. *Tectonophysics*, 11 (3): 175–190.

Zijderveld, J.D.A., 1967. A.C. demagnetization of rocks; analysis of results. In S.K. Runcorn (Editor), *Methods in Palaeomagnetism.* Elsevier, Amsterdam, pp. 254–286.